Stability Analysis of BLDC Motor Speed Controllers Under the Presence of Time Delays in the Control Loop

Julio C. G. Pimentel
Kylowave Incorporated
Ottawa, ON, CA
Email: jpiment@kylowave.com

Emad Gad
University of Ottawa
Ottawa, ON, CA
Email: egad@site.uottawa.ca

Sebastien Roy
Sherbrooke University
Sherbrooke, QC, CA
E-mail: Sebastien.Roy13@usherbrooke.ca

***Abstract*—This work discusses the stability issues of PI-based brushless DC motor (BLDCM) speed controllers under the presence of strong time delay in the controller loop. Understanding of the time delay effect is of paramount importance to increase performance, quality and productivity in important modern applications. Unfortunately, the time delay effect in the speed controller asymptotic stability has not been well studied in the existing literature.**

In this work, we present an algebraic technique to calculate the maximum time delay that can be accepted in the control loop of a BLDCM speed controller before the response becomes unstable. Initially, we derive an analytical model for the set point tracking (SPT) and the load disturbance rejection (LDR) responses taking into account the various sources of time delay. Using a recently proposed stability analysis methodology, we derive accurate stability conditions for the BLDCM speed controller. The results show that tuning the PI controller for very fast response causes the time delay to significantly affect the system stability. As an example, the asymptotic stability of the LDR of a sensored controller is analyzed. The method proposed here can be easily extended to analyze the stability of the SPT response and the stability of sensorless controllers such as the direct Back EMF.

***Keywords*—Stability, Electric Differential, Electric Vehicle, High Speed Spindle, Motor Control, BLDC, High Speed Motor.**

I. Introduction

In the last decade, the so called BLDC motor became widely used in a variety of applications because of its robust mechanical topology and simplicity of control, higher speed of operation, higher torque for the same power density and lower manufacturing cost compared to existing frequency and vector controlled AC drives. Thus, BLDCMs have become widely used in low power and high speed applications creating a need for efficient and low cost controllers [1] [2]. Currently, they are used in energy related applications such as hybrid vehicles integrated starter-generator, fuel pumps and electric differential [3] [4] [5], consumer appliances, computer numerical control and drilling tools, small hydro and wind energy generation and flywheel energy-storage systems [6] [7].

In order to achieve high operating speed, the BLDCM design often adopts a small motor frame and consequent small rotor inertia, phase resistance and inductance, which leads to high efficiency and fast electrical and mechanical dynamics. Therefore, these motors are capable of fast SPT and fast LDR on the order of milliseconds. Existing literature has shown that the delay introduced by the sensors, actuators, the discretization method and the plant itself can significantly affect the system stability. This problem becomes even more important when the system response time is on the same order of magnitude or smaller than the delay.

There is limited available information in the existing literature concerning the effect of time delays on the asymptotic stability of speed controllers. Its effect is especially important in mission-critical applications such as electric vehicles, aircrafts and health care applications where acceptable performance must be guaranteed at a large range of operating conditions and at reasonable cost. Traditionally, the time delay effect has been analyzed using classical methods based on Bode or Nyquist plots [8] [9]. These graphical methods are easy to use and provide some insight if one seeks the effect of a particular value of delay. Otherwise, they are rather inconvenient if one seeks to analyze a range of delay values as a plot would need to be constructed for each value of interest. The development of an algebraic asymptotic stability criterion would be much more convenient. Because of the difficulty involved in fully analyzing the effect of the time delays, motion control designers tend to adopt conservative tuning for the controllers, which is contradictory with the need for very high performance required by those applications.

Recently, some effort has been made to develop analytical methods that can be used for more general analysis in order to provide further insight into the overall system stability. These methods were developed using the Lyapunov functional stability theory. In [10], the authors analyze the stability of a novel BLDCM control scheme using Hall-effect switching technique to ensure closed-loop stable operation under various sets of loads, speeds, and input voltages. Reference [11] extends the previous work and derives a novel stability criterion that also considers the effect of the load torque. However, neither work considers the effect of the Hall sensor speed measurement delay in the overall system stability. It is noteworthy that a similar delay effect should also happen when a direct Back EMF sensorless method is used instead of a Hall sensor. These

methods use the back EMF voltage measured at the stator winding of the floating phase to detect the Back EMF zero-crossing point (ZCP). The ZCP can be used to estimate the rotor position and the inverter driver commutation controls by an additional shifting of 30^o. In case of a three-phase BLDCM, it produces 6 commutations per revolution [3].

In this work, we present an accurate analysis of a BLDCM speed controller stability under various speeds, load torques as well as contributions from various sources of time delays. We construct an analytic model with delays for the SPT and the LDR responses and use a recently presented time delay analysis method, initially proposed in [12], and later extended in [13], to derive the stability conditions under the presence of strong time delays, and compare the results to a commercial controller. By means of theoretical analysis, simulation and experimentation, we show that the conditions match the expected results. The paper is organized as follows: Section II briefly develops the BLDCM state-space model. Section III identifies various sources of delay affecting the controller stability and presents the development of the BLDCM models with time delays. Section IV presents a quick summary of the time delay analysis method used and derives the stability conditions. Finally, Section V presents the test bench built to validate the results including simulated and measured results.

II. BLDCM State Space Model

Modeling of BLDCMs has been well studied in the literature such that it is briefly presented here [1] [14] [15]. Assuming that the BLDCM of Figure 1 is symmetric in all three phases and that there is no change in the rotor reluctance with angle because of a non-salient rotor, its electrical circuitry model can be written as

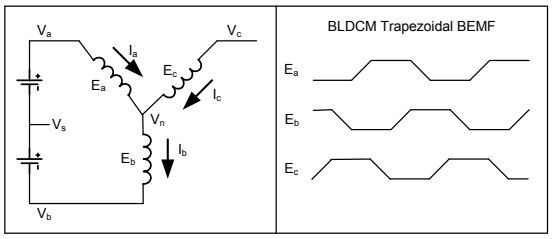

Fig. 1. BLDC Motor Electric Circuitry.

$$\begin{bmatrix} v_a \\ v_b \\ v_c \end{bmatrix} = \left(\begin{bmatrix} R_s & 0 & 0 \\ 0 & R_s & 0 \\ 0 & 0 & R_s \end{bmatrix} + \frac{d}{dt} \begin{bmatrix} L_s & 0 & 0 \\ 0 & L_s & 0 \\ 0 & 0 & L_s \end{bmatrix} \right) \begin{bmatrix} i_a \\ i_b \\ i_c \end{bmatrix} + \begin{bmatrix} e_a \\ e_b \\ e_c \end{bmatrix}, \quad (1)$$

where v_a, v_b, v_c, i_a, i_b and i_c are the motor phase voltage and currents respectively, P is the number of poles, L and M are the winding self and mutual inductance, $L_s = L - M$ and e_a, e_b and e_c are the induced BEMF voltages. In a PMM, the BEMF is a function of the rotor position and can be written as $e(\theta) = \lambda \omega_r f(\theta)$, where λ represents the total flux linkage and ω_r is the motor shaft rotational speed. For a BLDCM, $f(\theta)$ is a trapezoidal function with peak values at $+1$ and -1. For the sake of clarity, from now on we will henceforth omit the angle θ in the BEMF equation. The generated electromagnetic torque is given by (2). If J is the rotor moment of inertia, B_m is the viscous friction coefficient and T_l is the load torque, then the mechanical model can be written as follows:

$$T_e = \frac{e_a i_a + e_b i_b + e_c i_c}{\omega_r}, \quad (2)$$

$$J\frac{d\omega_r}{dt} + B_m \omega_r = T_e - T_l, \qquad \frac{d\theta}{dt} = \omega_r. \quad (3)$$

hence, the nonlinear state space model with $\boldsymbol{x}(t) = \begin{bmatrix} i_a & i_b & i_c & \omega_r \end{bmatrix}^T$ and $\boldsymbol{u}(t) = \begin{bmatrix} v_a & v_b & v_c & T_l \end{bmatrix}^T$ can be written as

$$\frac{\mathrm{d}\boldsymbol{x}(t)}{\mathrm{d}t} = \boldsymbol{A}\boldsymbol{x}(t) + \boldsymbol{B}\boldsymbol{u}(t), \quad (4)$$

$$\boldsymbol{y(t)} = \boldsymbol{C}\boldsymbol{x}(t), \quad (5)$$

$$\boldsymbol{A} = \begin{bmatrix} -R/L & 0 & 0 & \lambda f_a(\theta)/L & 0 \\ 0 & -R/L & 0 & \lambda f_b(\theta)/L & 0 \\ 0 & 0 & -R/L & \lambda f_c(\theta)/L & 0 \\ \lambda f_a(\theta)/J & \lambda f_b(\theta)/J & \lambda f_c(\theta)/J & -B_m/J & \end{bmatrix},$$

$$\boldsymbol{B} = \begin{bmatrix} 1/L & 0 & 0 & 0 \\ 0 & 1/L & 0 & 0 \\ 0 & 0 & 1/L & 0 \\ 0 & 0 & 0 & -1/J \end{bmatrix}.$$

Assuming the BLDC motor is phase-balanced and wye-connected then $i_a + i_b + i_c = 0$ and $v_s = \sum_{i=a}^{c} v_i - \sum_{i=a}^{c} e_i$. Note that the motor can be modeled by just two currents as the third current is dependent of the other two. From (2) to (4), we can derive the BLDCM non linear state space model with state variables i_a, i_b and ω_r as follows:

$$\boldsymbol{A} = \begin{bmatrix} -R/L & 0 & \lambda/3L(2f_a - f_b - f_c) \\ 0 & -R/L & \lambda/3L(2f_b - f_a - f_c) \\ \lambda/2J(f_a - f_c) & \lambda/2J(f_b - f_c) & -B_m/J \end{bmatrix},$$

$$\boldsymbol{B} = \frac{1}{3L} \begin{bmatrix} 2 & -1 & -1 & 0 \\ -1 & 2 & -1 & 0 \\ 0 & 0 & 0 & -3L/J \end{bmatrix}.$$

where the state variable $\boldsymbol{x}(t) \in \mathbb{R}^3$ is given by $\boldsymbol{x}(t) = \begin{bmatrix} i_a & i_b & \omega_r \end{bmatrix}^T$ and the input vector $\boldsymbol{u}(t) \in \mathbb{R}^4$ is given by $\boldsymbol{u}(t) = \begin{bmatrix} v_a & v_b & v_c & T_l \end{bmatrix}^T$. $\boldsymbol{A} \in \mathbb{R}^{3\times3}$, $\boldsymbol{B} \in \mathbb{R}^{3\times4}$ and $\boldsymbol{C} = \boldsymbol{I} \in \mathbb{R}^{3\times3}$ are the matrices describing the dynamics of the BLDCM continuous-time model (CTM). We can further simplify the model in (4). In a BLDCM, there are only two phases being driven at any time while the third phase is open. Assuming that $B_m \ll 0$ such that $B_m R \approx 0$ and $B_m L \approx 0$, and that phases a and b are driven by voltage sources v_a and v_b respectively, then $i_c = 0$ and $i_a = -i_b$. Therefore, the model in (4), with $k_e = 2\lambda$, $\boldsymbol{x}(t) = \begin{bmatrix} i_a & \omega_r \end{bmatrix}^T$, $\boldsymbol{u}(t) = \begin{bmatrix} (v_a - v_b) & T_l \end{bmatrix}^T$, can be rewritten as

$$\frac{\mathrm{d}\boldsymbol{x}(t)}{\mathrm{d}t} = \boldsymbol{A}_{2\times2}\boldsymbol{x}(t) + \boldsymbol{B}_{2\times2}\boldsymbol{u}(t), \quad (6)$$

$$\boldsymbol{y(t)} = \boldsymbol{C}_{2\times2}\boldsymbol{x}(t), \quad (7)$$

$$\boldsymbol{A}_{2\times2} = \begin{bmatrix} -R/L & -k_e/L \\ k_e/J & -B_m/J \end{bmatrix}, \qquad \boldsymbol{B}_{2\times2} = \begin{bmatrix} 1/L & 0 \\ 0 & -1/J \end{bmatrix}.$$

III. BLDCM Speed Controller With Loop Delays

Figure 2 presents the linearized model of a BLDCM speed controller showing various sources of delay in the control loop. Assuming the rotational speed ω_r is measured at every transition of all three Hall sensor signals, the delay τ_h introduced by the Hall sensor speed estimator is dependent on the shaft

speed ω_r and is given by $\tau_h = 2\pi/6\omega_r$. The discretization of the PI controller and the LPF CTMs introduces an additional discrete sampling time delay τ for each. In general, the mechanical dynamical responses of medium and large size motors running at moderate rotational speeds are much slower than the dynamics of the effects introduced by the delays. It is common design practice to ignore them without significantly sacrificing the controller's accuracy or performance. From Table I, we can see that small and high speed BLDC motors may have a mechanical time constant that is on the same order of magnitude as the loop delays shown in Figure 2. In many mission critical applications such as fuel pumps and electric differential in electrical vehicles [3] [4] [5], it is important to compensate load disturbance as fast as possible. These applications require the design of fast controllers with a short loop time. Therefore, those delays cannot be ignored and their effect on the overall system stability must be taken into account.

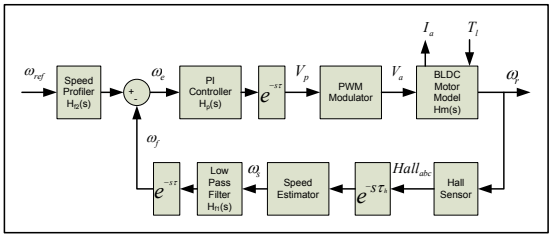

Fig. 2. BLDC motor speed controller with sources of delay.

TABLE I
BLDC MOTORS SPECIFICATION. (1) BL3056 (2) MAXON 118888 (3) MAXON 305013 (4) 500KRPM X 1KW PMSM (MEASURED IN REF. [16]).

Parameters	BLDC Motors				
	1	2	3	4	Unit
Num. of poles	2	2	4	1	
Rated speed	8.671	11.60	15.9	330	$kRPM$
Rated voltage	24.0	18.0	24.0	400	V
Rated power	28.96	50.05	103.2	1000	W
ph-ph resistance	2.3	0.573	0.102	0.5	Ω
ph-ph inductance	0.56	0.090	0.016	0.043	mH
BEMF constant	2.34	1.357	1.429	0.57*	mV/RPM
Torque constant	22.3	13.0	13.6	5.46*	$mN.m/A$
Elec. time cte	0.24	0.16	0.16	0.086	ms
Mech. time cte	7.4	6.82	1.82	26.67	ms
Rotor inertia	16.0	20.0	33.3	15.9	$g.cm^2$

When speed control of a motor with voltage amplifier (no current feedback) is desired, the plant can be modeled as a second order system. From (6) and using the linear transformation $\boldsymbol{H}(s) = \boldsymbol{C}_{2\times2}\left(s\boldsymbol{I} - \boldsymbol{A}_{2\times2}\right)^{-1}\boldsymbol{B}_{2\times2}$ and further assuming that $B_m \approx 0$, we can derive the BLDCM transfer function $\Omega_r(s) = H_m(s)V(s)$ between the terminal voltage $V(s) = V_a(s) - V_b(s)$ and the shaft rotational speed $\Omega_r(s)$ with $T_l = 0$ ig givn by (8). Defining the electrical and mechanical time constants as $\tau_{elec} = L/R$ and $\tau_{mech} = RJ/k_e^2$ respectively, we can rewrite (8) as (9). The PWM-modulated BLDCM driver transfer function $H_{pwm}(s)$ is given by (10).

$$H_m(s) = \frac{\Omega_r(s)}{V(s)} = \frac{1/k_e}{\frac{RJ}{k_e^2}\frac{L}{R}s^2 + \frac{RJ}{k_e^2}s + 1}. \quad (8)$$

$$H_m(s) = \frac{\Omega_r(s)}{V(s)} = \frac{1/k_e}{\tau_{mech}\tau_{elec}s^2 + \tau_{mech}s + 1} \quad (9)$$

$$H_{pwm}(s) = \frac{V_a(s)}{V_p(s)} = \frac{V_{dc}}{\tau_{pwm}s + 1},\ \tau_{pwm} = \frac{1}{2f_{pwm}}. \quad (10)$$

Generally, its PWM frequency is much higher than the controller sampling frequency such that $H_{pwm}(s) \approx V_{dc}$. The BLDCM electrical and mechanical part, the LPF and the the PI controller transfer functions H_{elec}, $H_{mech}(s)$, $H_{f1}(s)$ and $H_p(s)$, respectively, are given by (11) to (13).

$$H_{elec}(s) = \frac{I_a(s)}{V(s)} = \frac{1/R}{\tau_e s + 1},\ \tau_e = \frac{L}{R}, \quad (11)$$

$$H_{mech}(s) = \frac{\Omega_r(s)}{T_e(s) - T_l(s)} = \frac{1/B_m}{\tau_m s + 1},\ \tau_m = \frac{J}{B_m}, \quad (12)$$

$$H_{f1}(s) = \frac{\Omega_f(s)}{\Omega_s(s)} = \frac{k_{f1}}{\tau_{f1}s + 1}e^{-s\tau}, \quad (13)$$

$$H_p(s) = \frac{V_p(s)}{\Omega_e(s)} = k_p\frac{\tau_{iw}s + 1}{\tau_{iw}s}e^{-s\tau},\ \tau_{iw} = \frac{k_p}{k_i}. \quad (14)$$

where k_{f1} and τ_{f1} are the gain and the LPF time constant; k_p, k_i are respectively the proportional and the integral gains. τ_{iw} is the PI controller time constant. From control systems theory, we can easily see that the SPT transfer function $H_s(s)$ assuming that the load torque input $T_l = 0$ is given by

$$H_s = \frac{\Omega_r}{\Omega_{ref}} = \frac{H_p H_{pwm} H_m H_{f2} e^{-s\tau}}{1 + H_p H_{pwm} H_m H_{f1} e^{-s(2\tau+\tau_h)}}, \quad (15)$$

where the Laplace complex frequency s has been omitted for the sake of clarity. V_{dc} is the DC bus voltage of the PWM-modulated BLDCM driver and $H_{f2}(s)$ is the transfer function of the input speed profiler. Similarly, assuming that the rotational reference speed $\omega_{ref} = 0$, the LDR transfer function $H_l(s)$ between the load torque T_l and the BLDCM shaft rotational speed Ω_r is given by

$$H_l = \frac{\Omega_r}{T_l} = \frac{H_{mech}}{1 + k_e H_x + H_p H_{pwm} H_{f1} H_x e^{-s(2\tau+\tau_h)}}, \quad (16)$$

where $H_x = k_e H_{elec} H_{mech}$. The continuous-time delay τ_h (previously defined as $\tau_h = 2\pi/6\omega_r$) can only be sampled between two sampling times τ. Therefore, its contribution to the loop delay is given by $sup(\frac{\tau_h}{\tau})$. Looking at (15) and (16), we can notice that, in both transfer functions, all delay contributions are lumped together in the total delay $\tau_t = m\tau$ with $m = 2 + sup(\frac{\tau_h}{\tau})$. It is easy to see that the total delay τ_t is inversely proportional to the shaft rotational speed ω_r. In this work, we will assume that, in case of the LDR response, the variation caused to a steady-state speed ω_r by variations in the load torque T_l are sufficiently small such that the total delay τ_t can be considered to be constant. Therefore, the respective characteristic polynomials $C_{Hs}(s) = D(H_s(s))$

and $C_{Hl}(s) = D(H_l(s))$ are given by (17) and (18).

$$C_{Hs}(s) = k_s(\tau_{iw}s + 1)e^{-s\tau_t} + \tau_{iw}s(\tau_l s + 1)(\tau_{f1}s + 1) \quad (17)$$

$$C_{Hl}(s) = k_l(s\tau_{iw} + 1)e^{-s\tau_t} + sk_m(s\tau_{f1} + 1) + sk_n(s\tau_e + 1)(s\tau_m + 1)(s\tau_{f1} + 1) \quad (18)$$

where D denotes the denominators of $H_s(s)$ and $H_l(s)$, $k_s = \frac{k_p V_{dc}}{k_e}$, $k_l = \frac{k_p k_e k_{f1} V_{dc}}{R}$, $k_m = \tau_{iw}\frac{K_e^2}{R}$ and $k_n = B_m\tau_{iw}$. It is important to notice that (17) and (18) are two different retarded time delay systems (RTDS) with different roots and a single discrete delay τ_t [17] [18]. Therefore, the SPT and the LDR transfer functions have different stability conditions. Optimum performance can not be simultaneously achieved for both responses. Looking at (15) and (16), we can see that τ_t contributes differently to each of the characteristic polynomials. Thus, we should expect it to produce different effects in the stability of $H_s(s)$ and $H_l(s)$. In the following section, we will analyze the asymptotic stability of the speed controller LDR response $H_l(s)$ under the presence of the time-delay τ_t. The method presented here can be easily extended to analyze the stability of the SPT response $H_s(s)$ as well.

IV. Stability Analysis With Loop Delays

The work presented in [19] compares the performance of some of the most important methods to determine the imaginary characteristic roots of LTI retarded time delayed systems of the type of (18). To the best of the author's knowledge, this method has never been used to study the stability of BLDC motor drives. Reference [19] reports the method initially proposed in [12] and later extended in [13] and presents some important benefits compared to the other four tested methods. It produces a smaller degree for the crossing frequency polynomial and requires the search for real roots instead of complex ones as in the other methods. This is a great advantage as numerical roundoff errors make it very hard to calculate complex imaginary roots. As an example, we analyze here the asymptotic stability of the LDR response of a Hall-based sensored controller. However, the method proposed can be easily extended to analyze the stability of the SPT response as well and of sensorless controllers such as the direct Back EMF techniques. The procedure consists in deploying the following substitution proposed by Rekasius [20] and explained in [12]:

$$e^{-s\tau_t} = \frac{1 - sT}{1 + sT},\ \tau \in \Re^+,\ T \in \Re, \quad (19)$$

$$\tau_t = \frac{2}{\omega}\left[tan^{-1}(\omega T) \mp l\pi\right],\ l = 0, 1, 2, \ldots \quad (20)$$

Note that this equation is exact (not an approximation) and is defined only in $s = \omega i$, $\omega \in \Re$, with the obvious mapping condition of (20). Given a frequency ω, it describes an asymmetric mapping from one T value to an infinite number of τ_t's. Nevertheless, for the same τ_t there corresponds only one T. Substituting (20) in (18) and multiplying both sides of the equation by $(1 + sT)$, we obtain a new characteristic polynomial in s without the transcendental term $e^{-s\tau_t}$.

$$C_{Hl}(s,T) = k_l(s\tau_{iw} + 1)(1 - sT) + sk_m(s\tau_{f1} + 1)(1 + sT) + sk_n(s\tau_e + 1)(s\tau_m + 1)(s\tau_{f1} + 1)(1 + sT) \quad (21)$$

After some algebraic manipulation, we can rewrite (21) as

$$C_{Hl}(s,T) = b_5 s^5 + b_4 s^4 + b_3 s^3 + b_2 s^2 + b_1 s + b_0 \quad (22)$$

$$b_5 = k_n\tau_e\tau_m\tau_{f1}T$$

$$b_4 = k_n\tau_e\tau_m\tau_{f1} + (k_n\tau_e\tau_m + k_n\tau_e\tau_{f1} + k_n\tau_m\tau_{f1})T$$

$$b_3 = k_m\tau_e\tau_m + k_n\tau_e\tau_{f1} + k_n\tau_m\tau_{f1} + (k_m\tau_{f1} + k_n\tau_e + k_n\tau_m + k_n\tau_{f1})T$$

$$b_2 = k_m\tau_{f1} + k_n\tau_e + k_n\tau_m + k_n\tau_{f1} + (k_m + k_n - k_l\tau_{iw})T$$

$$b_1 = k_l\tau_{iw} + k_m + k_n - k_eT \qquad b_0 = k_l$$

Equation (22) is the general form of the characteristic polynomial of the speed controller of Figure 2, where the transcendental exponential term has been removed by the Rekasius mapping. $C_{Hl}(s,T)$ is a polynomial in s with parameterized coefficients in T. The next step consists in determining all values of $T \in \Re$ which cause imaginary roots of type $s = \omega i$. This can be achieved by following the procedure explained in detail in [19] and [12] and summarized here:

1) Form the Routh-Hurwitz array (RHA) of (22), set the term in the s^1 row to zero and calculate the roots T_{cr} corresponding to the imaginary crossing frequencies.
2) The corresponding crossing frequencies $s = \omega i$ can be found using the auxiliary equation formed by the s^2 row of the RHA Notice that the s^2 row has two terms which are functions of T. Check that their sign agree such that the corresponding T values yield imaginary frequencies.
3) Check whether there are degenerate imaginary roots at the origin ($s = \omega i$ with $\omega = 0$) by checking the constant term in (22) with no s term. If $\sum_{k=0}^{p} a_k(0) = 0$ is satisfied (where $a_k(s)$ are the polynomials in s of 18), there is at least one root at $s = 0$.
4) Search for imaginary roots when $T = \mp\infty$. In this case, $e^{-s\tau_t} \to -1$ and $C_{Hl}(s,T)$ becomes a simple polynomial in s. If any root of this polynomial is purely imaginary, it also becomes part of the solution.
5) Compute the root tendency RT of (23) which represents the direction of the transition of the roots crossing the imaginary axis to the unstable RHP ($RT = +1$) or to the stable LHP ($RT = -1$), where n is the order of the commensurate delays. Equation (18) has a single delay τ_t such that $n = 1$ [12].

$$RT = sgn\left[img\left(\frac{\sum_{j=0}^{n} a'_j e^{-j\tau_t s}}{\sum_{j=0}^{n} j a_j e^{-j\tau_t s}}\right)\right], \quad (23)$$

V. Experimental Results

The testbench includes a Stellaris BLDC motor control reference design kit (RDK-BLDC) and a Xilinx University Program Virtex-II Pro Development Board. The BLDCM

model and PI-based speed controller were simulated in Matlab/Simulink V2010a. The Stellaris kit comes with a Beijing Motors BL3056 BLDC motor. Its shaft was connected through a coupler to the shaft of a 24 Vdc DC motor operating in generator mode. The generator stator was connected to various resistive loads through an array of power switches. This structure allowed us to quickly connect and disconnect loads to the generator, creating accurate transient torque scenarios with good accuracy and repeatability. Table II shows the parameters used for the PI-controller k_p and k_i parameters. The objective was, for a given BLDCM, to study how the PI controller tuning affects the time delay range of stability. An ad-hoc approach was used to tune the PI controller to two aggressive operating points. AdHoc1 k_p and k_i parameters were chosen to place the system transient response at the limit of stability. AdHoc2 k_p and k_i values were chosen to also provide an aggressive tuning albeit more conservative than AdHoc1 in order to generate a fast and stable transient response. The TI entry show the default values used in the Stellaris RDK-BLDC kit.

TABLE II
PI CONTROLLER PARAMETERS CALCULATED BY VARIOUS METHODS.

Parameter	Tuning Method			
	TI	AdHoc2	AdHoc1	Symbol
Samp. time (ms)	1.0	1.0	1.0	T_s
PI k_p $(x10^{-4})$	1.22	4.679	1.22	k_p
PI k_i $(x10^{-4})$	3.66	633.5	1708	k_i
PI time cte (ms)	333	7.39	0.715	τ_{iw}
τ_{iw}/τ_m Ratio	45	0.998	0.097	k_τ

Consider the BLDC motor 1 of Table I. Applying test conditions above on the characteristic polynomials (18) and (22) and using the TI Stellaris PI controller parameters, we observe the following results:

1) Setting the RHA term s^1 to zero produces two conjugate pairs of roots (which are discarded) and the following real roots: $T_{cr} = (-0.0040071, -0.0002207, 2.8666189)$.
2) Using row s^2 of the RHA, we obtain the following crossing frequencies: $\omega_r = (6.9915, 0.3976)$. Note that root $T_{cr} = 2.8666189$ produces an ω_r approaching zero and was discarded.
3) Given that $\sum_{k=0}^{p} a_k(0) \neq 0$, it follows that $C_{Hl}(s)$ has no degenerated imaginary roots at the origin.
4) When $T = \mp\infty$ we have $C_{Hl}(s,T) = -k_l(s\tau_{iw}+1) + sk_m(s\tau_{f1}+1) + sk_n(s\tau_e+1)(s\tau_m+1)(s\tau_{f1}+1)$. Hence, $C_{Hl}(s,T)$ does not admit any purely imaginary roots.
5) Finally, the root tendency is computed as: $RT = (-1, 1)$. These results lead to the following critical delay values: $T_{au} = (0.8982, 4.2789)$. Because the polynomial has no unstable roots at $\tau_t = 0$, and the first $RT = -1$ implies a transition to the RHP, the only stable time delay interval is the range between 0 and 0.8982.

The algorithm presented in Section IV was coded in Matlab $m-language$. Using k_p and k_i parameters of Table II, the electrical parameters of the TI Stellaris BLDCM, a digital LPF with cutoff frequency of $\omega_{f1} = 287.7\ rad/s$, BLDCM rotational speed ω_r of 6 $kRPM$ and 1 $kRPM$, and sampling time $T_s = 1\ ms$, the proposed algorithm provided the maximum control loop time delay $\tau_t(max)$ estimates shown in Table III. From the same table, we see that the control loop time delay at 6 $kRPM$ and 1 $kRPM$ is 3.7 ms and 12.0 ms respectively. As we can see, the TI Stellaris controller has adopted an extremely conservative PI controller which produces the sluggish transient response shown in Figure 3 and confirmed by the experimental results in Figures 4 and 5.

TABLE III
ESTIMATED TIME DELAY INTERVALS.

Parameter	Tuning Method		
	TI	AdHoc2	AdHoc1
$\tau_t(max)$ (ms)	898	24.1	7.3
τ_t@$6KRPM$ (ms)	3.7	3.7	3.7
τ_t@$1KRPM$ (ms)	12.0	12.0	12.0
G. Margin@$6kRPM$	56.5	53.84	0.59
P. Margin@$6kRPM$	82.7	53.55	4.39
G. Margin@$1kRPM$	58.4	61.64	8.26
P. Margin@$1kRPM$	82.0	29.67	-82.1

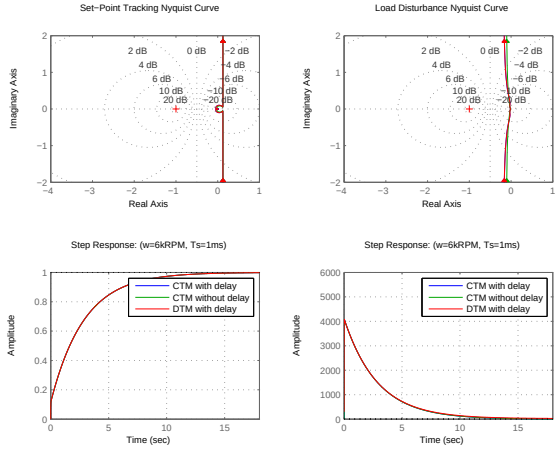

Fig. 3. Delay Effect Using TI tuning values at $\omega_r = 1kRPM$.

The values adopted for k_p and k_i allow the controller to handle control loop time delays on the order of hundreds of milliseconds, albeit at the expense of very slow dynamical responses. The extremely aggressive tuning of AdHoc1 produces a fast transient response that is very close to instability for 6 $kRPM$ and unstable for 1 $kRPM$, as predicted by the proposed method. Finally, the AdHoc2 tuning values produce very fast transient responses and very stable behavior at 6 $kRPM$. However, as the rotational speed ω_r decreases to 1 $kRPM$, the phase margin starts to approach critical levels and we should expect some oscillatory behavior. These results are confirmed by the Nyquist plot and the step responses shown in Figures 6 and 7.

VI. CONCLUSION

This work presented an effective technique to analyze the algebraic asymptotic stability of a BLDCM speed controller with strong time delays. The new approach is based on an

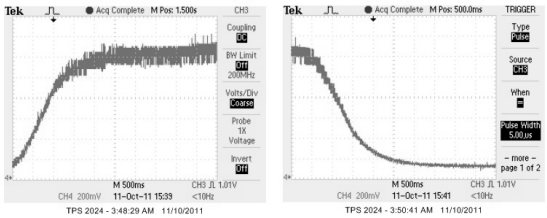

Fig. 4. Speed transient from 1000 to 6000 RPM at no load.

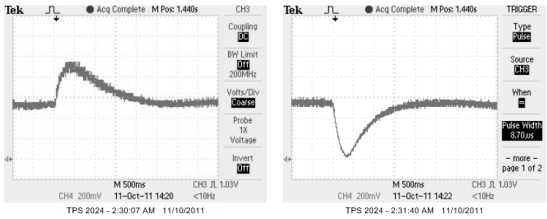

Fig. 5. Torque transient test at 3000 RPM (0 - 27.8 m NM - 0).

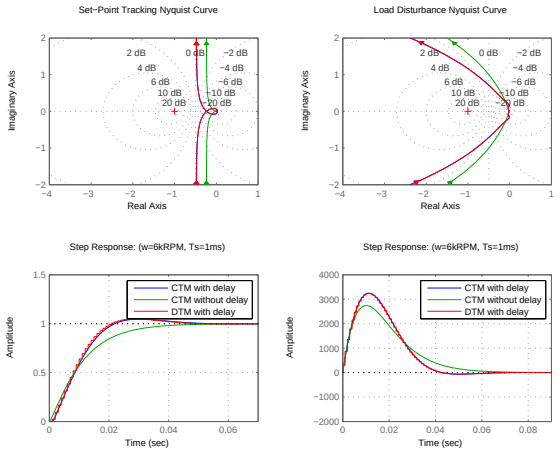

Fig. 6. Delay Effect Using AdHoc2 tuning values at $\omega_r = 6kRPM$.

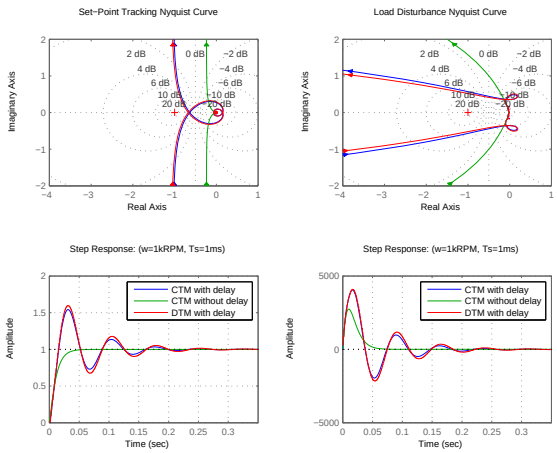

Fig. 7. Delay Effect Using AdHoc2 tuning values at $\omega_r = 6kRPM$.

algebraic method and is particularly useful to analyze the effect of a range of delay values. The proposed method contributes to the improvement of the robustness of high speed controllers by producing an explicit expression for the stability range for the total time delay in the controller loop. In the near future, we plan to extend the current results to others types of electrical machines.

ACKNOWLEDGMENT

This research work was supported in part by the NSERC/Engage and the NRC/IRAP Programs.

REFERENCES

[1] C.-L. Xia, *Permanent Magnet Brushless DC Motor Drives and Controls*. Beijing, China: Wiley Press, 2012.

[2] R. Ktrishman, *Permanent Magnet Synchronous and Brushless DC Motor Drives*. Florida, USA: CRC Press, 2009.

[3] T. W. Chun, Q. V. Tran, H. H. Lee, and H. G. Kim, "Sensorless control of bldc motor drive for an automotive fuel pump using a hysteresis comparator," *IEEE Trans. in Power Electronics*, vol. 29, pp. 1382–1391, March 2014.

[4] D. Collins, P. Anderson, S. Beyer, and D. Moreno, "Brushless motors for in-tank fuel pumps," in *Proceedings of the SAE 2012 World Congress & Exhibition*, (PA, USA), SAE International, Apr 2012.

[5] M. Gougani, M. Chapariha, J. Jatskevich, and A. Davoudi, "Hall sensor-based locking electric differential system for bldc motor driven electric vehicles," in *Proceedings of IEEE International Electric Vehicle Conference (IEVC2012)*, (NJ, USA), pp. 1–7, IEEE, March 2012.

[6] A. Vanisri and N. Devarajan, "Torque ripple minimization in indirect position detection of permanent magnet brushless dc motor," *European Journal of Scientific Research*, vol. 65, pp. 481–489, Dec. 2011.

[7] Z. Kolondzovski, A. Arkkio, J. Larjola, and P. Sallinen, "Power limits of highspeed permanent magnet electrical machines for compressor applications," tech. rep., Aalto Univ., School of Science and Tech., 2010.

[8] G. F. Franklin, P. J. D., and W. M., *Digital Control of Dynamic Systems*. Addson-Wesley, 3 ed., 1998.

[9] K. Ogata, *Discrete-Time Control Systems*. Prentice-Hall, 2 ed., 1995.

[10] N. Milivojevic, M. Krishnamurthy, Y. Gurkaynak, A. Sathyan, Y.-J. Lee, and A. Emadi, "Stability analysis of fpga-based control of brushless dc motors and generators using digital pwm technique," *IEEE Transactions on Industrial Electronics*, vol. 59, pp. 343–351, Jan 2012.

[11] A. Tashakori and M. Ektesabi, "Stability analysis of sensorless bldc motor drive using digital pwm technique for electric vehicles," in *IECON 2012 - 38th Annual Conference on IEEE Industrial Electronics Society*, (NJ, USA), pp. 4898 – 4903, IEEE, Oct 2012.

[12] N. Olgac and R. Sipahi, "An exact method for the stability analysis of time delayed lti systems," *IEEE Transactions on Automatic Control*, vol. 47, pp. 793–797, May 2002.

[13] N. Olgac and R. Sipahi, "A practical method for analyzing the stability of neutral type ltitime delayed systems," *Automatica*, vol. 40, pp. 847–853, May 2004.

[14] M. G. Simoes and P. V. Jr., "A high-torque low-speed multiphase brushless machine - a perspective application for electric vehicles," *IEEE Trans. on Industrial Electronics*, vol. 49, pp. 1154–1164, Aug 2002.

[15] S. Kim, "Modeling and fault analysis of bldc motor based servo actuators for manipulators," in *IEEE International Conference on Robotics and Automation - ICRA*, pp. 767–772, May 2008.

[16] C. Zwyssig, D. Duerr, M. Hassler, and J. W. Kolar, "An ultra-high-speed, 500000 rpm, 1 kw electrical drive system," in *PCC'07*, (Nagoya, JP), pp. 1577–1583, Apr. 2007.

[17] K. Gu, V. L. Kharitonov, and J. Chen, *Introduction to Time-Delay Systems*. Boston, USA: Birkhauser, 2003.

[18] S. I. Niculescu and K. Gu, *Advances in Time-Delay Systems*. Berlin, Germany: Springer Verlag, 2004.

[19] R. Sipahi and N. Olgac, "A comparative survey in determining the imaginary characteristic roots of lti time delayed systems," in *Proceedings of the 16th IFAC World Congress, 2005*, (Laxenburg, AT), pp. 635–635, Elsevier IFAC, Jul 2005.

[20] Z. V. Rekasius, "A stability test for systems with delays," in *Proc. of Joint Automatic Control Conference*, (San Francisco, CA, USA), 1980.